

Simplified flexibility analysis of proteins

Yves-Henri Sanejouand*

UFIP, FRE-CNRS 3478, Faculté des Sciences et des Techniques, Nantes, France.

PACS numbers: 87.15.He; 87.15.-v; 46.40.-f

Keywords: Normal mode analysis, elastic network model, conformational change, B-factors, robust modes.

Abstract

A simple way to get insights about the possible functional motions of a protein is to perform a normal mode analysis (NMA). Indeed, it has been shown that low-frequency modes thus obtained are often closely related to domain motions involved in protein function. Moreover, because protein low-frequency modes are known to be robust, NMA can be performed using coarse-grained models. As a consequence, it can be done for large ensembles of conformations as well as for large systems, like the ribosome, whole virus capsids, *etc.* Unexpectedly, on the high-frequency side, modes obtained with cutoff-based coarse-grained models also seem able to provide useful insights on protein dynamical properties.

I. INTRODUCTION

In order to understand the function of a protein, the knowledge of its structure is of utmost importance. However, it is becoming more and more clear that in most cases this is not enough and that the relevant information needed is its *structural ensemble*, that is, a fair sample of the set of conformations a protein can visit at room temperature.

A straightforward way to obtain this information is to perform a *long enough* molecular dynamics (MD) simulation in explicit solvent. In practice, noteworthy in the case of enzymes, the timescale that has to be reached is at least of the order of the microsecond since the most efficient enzymes, like catalase, have turn-overs of this order of magnitude. Nowadays, for standard size proteins, MD simulations that long are routinely performed on supercomputers. Actually, using a dedicated ASICS-based supercomputer, the millisecond timescale has recently been reached, in the case of the small BPTI model system [1]. Moreover, starting from random initial configurations, accurate *ab initio* folding of several fast-folding peptides has been obtained [1, 2], revealing all the potential of the brute force approach for the years to come.

However, even with a supercomputer, obtaining the relevant structural ensemble through this approach often takes months. Moreover, this can hardly be done for very large systems, like the ribosome, whole virus capsids, *etc.*

So, simplified methods are still welcome, noteworthy because, as a consequence of their low computational cost, they can be implemented on web-servers, where anybody can give them a try.

II. NORMAL MODE ANALYSIS

A. Background

A simple way to study the flexibility of a molecule is to perform a normal mode analysis (NMA). This method rests upon the fact that the classical equations of motion for a set of N atoms can be solved analytically when the displacements of the atoms in the vicinity of their equilibrium positions are small enough. As a consequence, V , the potential energy of the studied system, can be approximated by the first terms of a Taylor series. Moreover, because the system is expected to be at equilibrium [62], the term with the first derivatives of the energy (the forces) can be dropped, so that:

$$V = \frac{1}{2} \sum_{i=1}^{3N} \sum_{j=1}^{3N} \left(\frac{\partial^2 V}{\partial r_i \partial r_j} \right)_0 (r_i - r_i^0)(r_j - r_j^0) \quad (1)$$

where r_i is the i^{th} coordinate of the system, r_i^0 being its equilibrium value.

In other words, within the frame of this approximation, the potential energy of a system can be written as a quadratic form. In such a case, it is quite straightforward to show that the equations of atomic motion have the following solutions [3, 4]:

$$r_i(t) = r_i^0 + \frac{1}{\sqrt{m_i}} \sum_{k=1}^{3N} C_k a_{ik} \cos(2\pi\nu_k t + \Phi_k) \quad (2)$$

where m_i is the atomic mass and where C_k and Φ_k , the amplitude and phasis of the so-called normal mode of vibration k , depend upon the initial conditions, that is, upon atomic positions and velocities at $t = 0$.

In practice, ν_k , the frequency of mode k , is obtained through the k^{th} eigenvalue of the mass-weighted Hessian of the potential energy, that is, the matrix whose elements are the mass-weighted second derivatives of the energy, the a_{ik} 's being the coordinates of the corresponding eigenvector.

In Fig. 1, the frequency spectrum thus obtained for the protease of human immunodeficiency virus (HIV)

*Electronic address: yves-henri.sanejouand@univ-nantes.fr

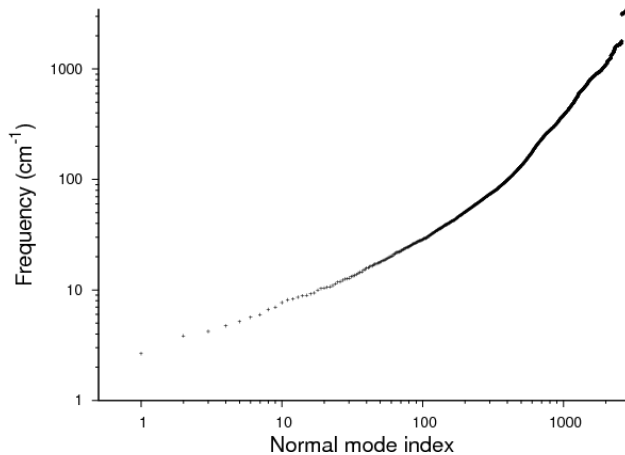


Figure 1: Spectrum of the HIV protease, as obtained using standard normal mode analysis. The structure considered is the monomer found in PDB 1HHP, after energy-minimization. High-frequency modes are localized motions of chemically bonded atoms. The highest-frequency ones correspond to motions in which a hydrogen atom is involved. There are only a few (164) of them because an extended-atom model was considered [6].

is shown, when a standard empirical energy function is used, namely, as available in CHARMM [5]. The modes with the highest frequencies correspond to motions of pairs of atoms that are chemically bonded and the reason why these frequencies are much higher than others is because a hydrogen (*i.e.*, a light particle) is involved in these bonds. Generally speaking, modes with high frequencies are localized, that is, only a few atoms are moving significantly at these frequencies.

On the contrary, on the low-frequency part of the spectrum, modes tend to involve large parts of the structure. This is probably why their comparison with protein functional motions was undertaken, the latter being often described as relative motions of structural domains [7]. As a matter of fact, in the first NMA study of a protein with well defined domains, namely, the human lysozyme, the lowest-frequency mode ($\nu_1 = 3.6 \text{ cm}^{-1}$) was found to correspond to a hinge-bending motion [8]. Later on, the lowest frequency modes of citrate synthase [9] and haemoglobin [10] were indeed found able to provide a fair description of the rather complex and large-amplitude motion these proteins experience upon ligand binding.

B. Technical issue

Getting the eigenvalues and eigenvectors of a large matrix can prove challenging, in particular because methods available in mathematical libraries usually require the storage of the whole matrix in the computer memory. For a small protein like monomeric HIV protease (99 residues), this is not an issue since, with an extended-atom model, the storage of its Hessian takes $\approx 10 \text{ Mo}$.

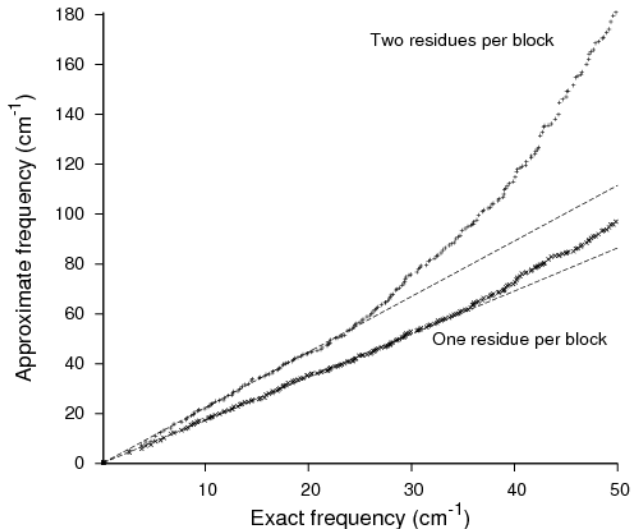


Figure 2: Approximate frequencies of the HIV protease, as obtained through the RTB approximation, as a function of exact ones, when one or two amino-acid residues are put in each block. Dotted lines are linear fits for the lowest-frequencies.

For dimeric citrate synthase (2×450 residues), it takes 3 Go. Twenty years ago, this used to be an issue [9]. It is not any more. However, for not so uncommon multimeric systems like aspartate transcarbamylase (nearly 3,000 residues), using standard approaches would still require to have access, like at the time [11], either to smarter numerical methods and/or to supercomputers, as the storage of the whole Hessian would take 30 Go of computer memory.

C. Useful methods and approximations

To overcome this practical limitation, several methods have been proposed. Note that within the frame of most of them it is not possible to get the $3N$ normal modes of the system, that is, its full spectrum.

When a good enough guess of a required eigenvector can be done, for instance when it is expected to be a relative motion of well-defined structural domains, a method of choice is the Lanczos one, especially because it only involves calculations of matrix-vector products. This method was applied to the case of human lysozyme [8] as well as, later on, using a more sophisticated version of the algorithm, to the case of dimeric citrate synthase [9].

Other methods usually rely on the splitting of the Hessian into blocks [12, 13], and/or on the choice of new coordinates that allow for the building of a smaller Hessian whose eigensolutions are as close as possible to the original ones [14]. For instance, the principle of the RTB approximation [15] is to use the six rotation (R) and translation (T) vectors of "blocks" (B) of atoms as the new set of coordinates [63]. When each block contains

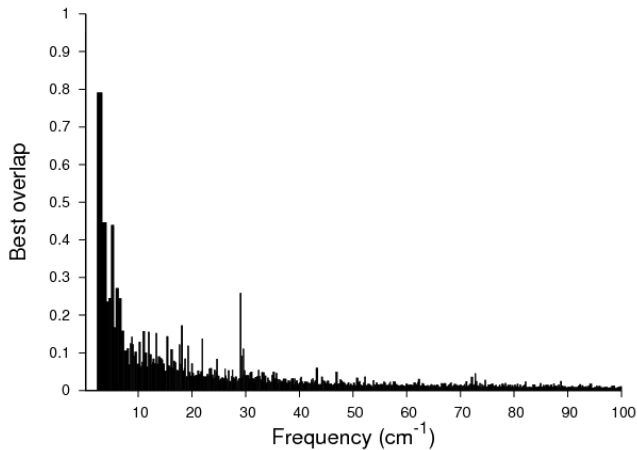


Figure 3: For each eigenvector of the HIV protease, as obtained using a standard empirical energy function, the best overlap with an eigenvector obtained using Tirion’s model is given. The structure considered is the monomer found in PDB 1HHP, after energy-minimization. Tirion’s model was built using $R_c = 5\text{\AA}$.

a whole amino-acid residue, since there is, on average, ≈ 16 atoms (48 coordinates) per residue, the order of the Hessian is reduced by a factor of ≈ 8 . Interestingly, if the frequencies calculated with this approximation are found to be, as expected, higher than those of the full Hessian, on the low-frequency part of the spectrum a proportionality is observed between approximate and exact values [16] (Fig. 2). Moreover, the corresponding approximate eigenvectors are found to be remarkably similar to exact ones [15, 16]. Of course, several amino-acid residues can be put in a given block [15], and the way atoms are grouped into blocks can be made on smarter grounds [17, 18].

Note that reducing the size of the Hessian is a coarse-graining process, which has the advantage of preserving the interactions between blocks, as they are observed in the all-atom model. On the other hand, the fact that low-frequency modes are little perturbed by the process suggest that they are robust, in the sense that the corresponding pattern of displacements does not depend significantly upon the details of the description of the system.

III. NETWORK MODELS

A. Tirion’s model

The fact that an approximation like (1) can prove useful for the study of protein functional motions is far from being obvious. First, because NMA is usually performed for a single minimum of the potential energy surface, while it is well known that at room temperature a protein explores a huge number of different ones [19]. More

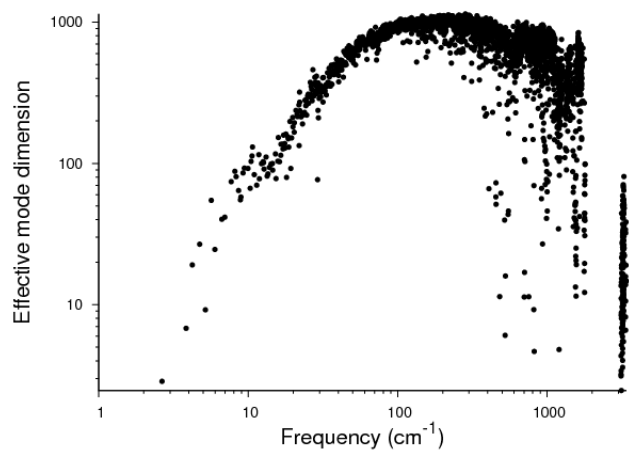


Figure 4: For each eigenvector of the HIV protease, as obtained using a standard empirical energy function, its dimension, *i.e.*, the effective number of Tirion’s eigenvectors involved in its description is given. The structure considered is the monomer found in PDB 1HHP, after energy-minimization. Tirion’s model was built using $R_c = 5\text{\AA}$.

generally, (1) means that the system is studied as if it were a solid, while it is quite clear that the liquid-like character of the dynamical behaviour of a protein, noteworthy of its amino-acid sidechains [20], is required for its function [21].

Moreover, prior to the development of simple implicit solvent models like EEF1 [6], NMA was usually performed *in vacuo*, while it is well known that water is essential for protein function [64], not to mention the significant distortion a system experiences during the required preliminary energy minimization, when solvent effects are only taken into account through an effective dielectric constant [22].

So, from the very beginning, the usefulness of NMA in the field of protein dynamics had to mean that functionally relevant normal modes are robust ones, similar from a minimum of the energy function to another [23, 24], but also from a forcefield to another. As an extreme check of the later point, Monique Tirion proposed to replace electrostatics and Lennard-Jones interactions in a protein by an harmonic term such that:

$$V_{nb} = \frac{1}{2}k_{enm} \sum_{d_{ij}^0 < R_c} (d_{ij} - d_{ij}^0)^2 \quad (3)$$

where d_{ij} is the actual distance between atoms i and j , d_{ij}^0 being their distance in the studied structure [25]. In other words, in Tirion’s model, all pairs of atoms less than R_c Ångströms away from each other are linked by Hookean springs. Note that when, as herein, k_{enm} , the force constant, is the same for all atom pairs, it only plays the role of a scaling factor for the frequencies of the system. As a corollary, the only parameter of the model is R_c .

To evaluate how similar modes obtained with such a

description of the non-bonded interactions in a protein are to those obtained with a standard, empirical, one, a useful quantity is the overlap:

$$O_{ij} = \left(\sum_k^{3N} a_{ki} a_{kj} \right)^2 \quad (4)$$

i.e. the square of the scalar product of the eigenvectors obtained in both cases. Note that, because eigenvectors are normalized, for each of them: $\sum_j^{3N} O_{ij} = 1$.

As shown in Fig. 3, the overlap between an eigenvector obtained with (3) and an eigenvector obtained with the energy function available in CHARMM [6], can be as high as 0.8, like in the case of the lowest-frequency mode of the HIV protease. So, obviously, this mode is a very robust one, in the sense that it depends little upon the nature of the atomic interactions in the structure. Note in particular that, in the simplified version of Tirion's model considered herein, at variance with Tirion's original work [25], chemically bonded atoms are treated on the same footing as other pairs of close atoms, that is, by linking them with a spring of same force constant (k_{enm}).

In the HIV protease case, only three low-frequency modes have an overlap with a mode obtained using Tirion's model that is larger than 0.4. However, this does not necessarily mean that HIV protease has only three highly robust modes, in particular because a given subset of modes can prove robust as a whole, even when each of them is not. To quantify this, D_i , the dimension of standard mode i , *i.e.*, the effective number of Tirion's modes involved in its description, can be calculated as follows [26, 27]:

$$D_i = \exp\left(-\sum_j^{3N} O_{ij} \log O_{ij}\right) \quad (5)$$

For the lowest-frequency mode of the HIV protease, $D_1 = 2.8$ and, indeed, as shown in Fig. 4, on the low-frequency side of the spectrum only three standard modes of the HIV protease can be described accurately with less than 10 Tirion's modes. However, three other ones can be described with less than 30 of them. Note also that some high-frequency modes can be described with a handful of Tirion's modes. This is because atomic masses are taken into account in Tirion's model. As a consequence, within the frame of this model also, high-frequency modes are well localized and, likewise, they correspond to localized motions in which hydrogen atoms are involved.

B. Proteins as undirected graphs

Describing interactions between amino-acid residues in terms of short-range harmonic springs (with, *e.g.*, $R_c=5\text{\AA}$), as proposed by Monique Tirion, and ending with a subset of low-frequency modes that are highly similar to those obtained with a much more complex description, suggests that such modes are due to some generic property.

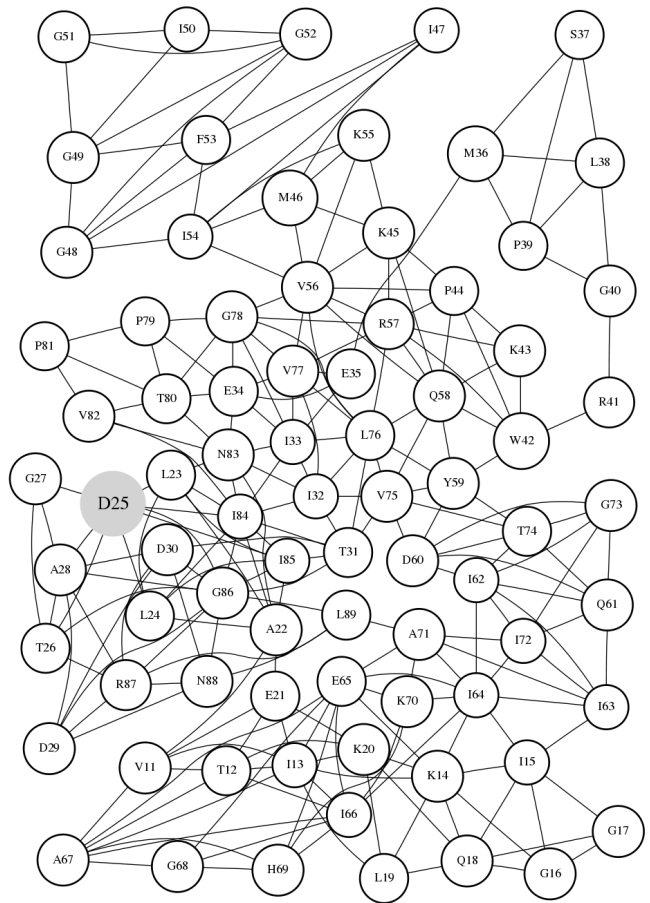


Figure 5: Graph of the interactions between HIV-protease residues. The catalytic residue (Asp 25) is indicated in grey. For the sake of clarity, the ten first and last residues were omitted. Drawn with Graphviz-Neato.

A possibility is that what determines the nature of these modes is the pattern of interactions between residues. As a matter of fact, simple methods have been proposed for evaluating protein flexibility through the study of the graph corresponding to the set of interactions observed in a given structure (Fig. 5 shows such a graph, in the case of the HIV protease). For instance, it has been shown that, using the highly efficient pebble game algorithm [28], hinges and flexible loops can be identified in proteins like the HIV protease, adenylate kinase, *etc* [29]. On the other hand, diagonalizing directly the corresponding, so-called adjacency, matrix provides fair estimates of the amplitude of atomic fluctuations, as observed experimentally, noteworthy through crystallographic Debye-Waller factors [30, 31] (see Section III E).

Interestingly, while the small eigenvalues of the adjacency matrix are enough for providing such estimates, large eigenvalues seem also able to provide useful informations. Indeed, because eigenvectors corresponding to large eigenvalues pinpoint spots in the structure where residue density (in a coarse-grained sense) is the highest, it has been suggested that they may correspond to

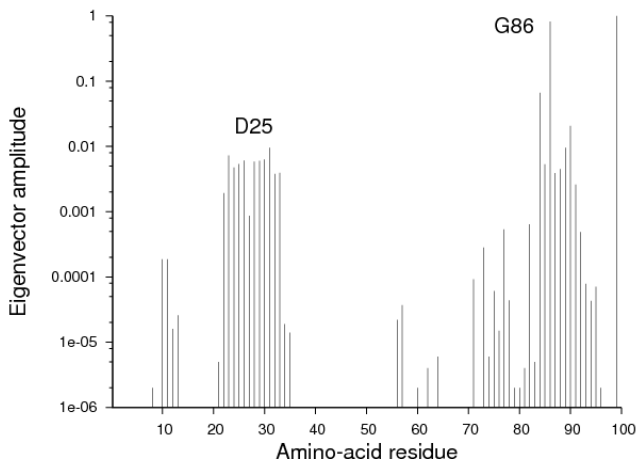


Figure 6: Eigenvector of the adjacency matrix of the HIV-protease (PDB 1HHP), corresponding to the largest eigenvalue. Here, two residues are defined as interacting ones (*i.e.*, the corresponding matrix element is -1) when the distance between their C_α is less than 6.5\AA . Note the logarithmic scale.

protein folding cores [32].

For instance, in the case of the HIV protease [32], the eigenvector corresponding to the largest eigenvalue is dominated by the motion of Gly 86 (Fig. 6) a residue close to Asp 25, the catalytic residue (see Fig. 5). As a matter of fact, there is an hydrogen-bond between the backbone carbonyl oxygen of the previous residue, Ile 85, and the backbone amide nitrogen of Asp 25. The fact that, in such a small protein, the folding core could prove that close to the enzyme active site would make sense, since enzymatic activity usually requires a precise positioning of the residues involved in the catalytic mechanism, that is, a rather rigid local environment.

C. Elastic Networks

However, by considering a protein as a graph, an important information is lost, namely, the directionality of the motions. This is probably why, among the family of simple protein models, 3D-Elastic Network models (ENM) seem to be the most popular ones. Such models are just one simplification step further from Tirion's model: here, residues are described as beads, often a single one, as initially proposed [34], although beads can also represent groups of residues [35], as well as whole protein monomers [36].

Using as beads the C_α atoms (C_α -ENM), it was shown that a few low-frequency modes of the coarse-grained elastic networks thus obtained are enough for describing accurately the motion a protein experiences upon ligand binding [27, 37, 38], as long as a significant portion of the protein is involved [27] (*e.g.*, whole domains), at least when the amplitude of the motion is large enough [39] (typically, more than $\approx 2\text{\AA}$ of C_α -rmsd [65]).

To measure how well normal mode i describes a given motion, a useful quantity is I_i , its involvement coefficient [9, 22]:

$$I_i = \left(\sum_j^{3N} a_{ji} \frac{\Delta r_j}{|\Delta r|} \right)^2 \quad (6)$$

where $\Delta \vec{r} = \vec{r}_b - \vec{r}_a$, \vec{r}_a and \vec{r}_b being the atomic positions observed in conformations a and b , respectively. Note that in order to have meaningful involvement coefficients, conformation b needs to be fitted onto conformation a , if the normal modes were obtained for the later. Note also that (6) is the square of the scalar product between $\Delta \vec{r}$ and normal mode i . So, as a consequence of normal modes orthogonality: $\sum_i^{3N} I_i = 1$. In other words, I_i gives the fraction of the protein motion that can be described just by considering the displacement of the system along mode i .

$\sum_i^n I_i$, the quality of the description of the closure motion of guanylate kinase (Fig. 7), as a function of n , the number of modes taken into account, is shown in Fig. 8, for the modes of the C_α -ENM built with an open form ($R_c = 10\text{\AA}$). In this case, which is far from being an exceptional one [27, 38], the lowest-frequency mode is enough for describing 72% of the functional motion ($I_1 = 0.72$). Note that such a high value of the involvement coefficient means that both patterns of atomic displacements are remarkably similar (Fig. 9). Indeed, the main difference concerns the relative amplitude of the motion of helices 125-135 and 141-157. On the other hand, together, modes three to five are able to describe 13% of the motion ($I_3 = 0.04$, $I_4 = 0.05$, $I_5 = 0.04$). So, four modes *only* are enough for describing 85% of the closure motion of guanylate kinase (8).

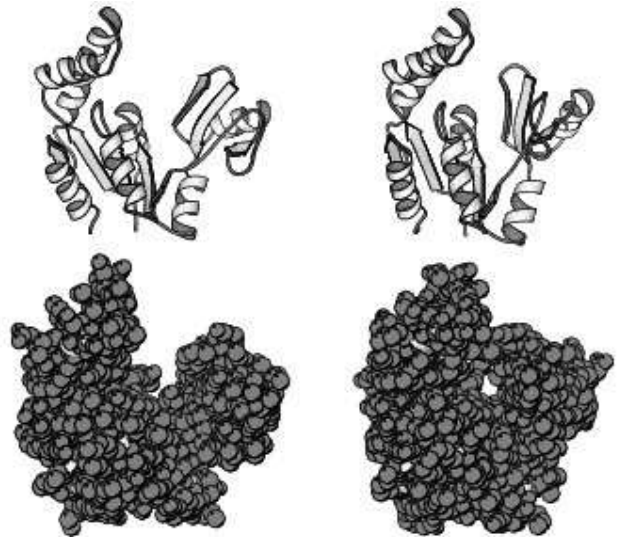


Figure 7: Conformational change of *Saccharomyces cerevisiae* guanylate kinase. Left: open form (PDB 1EX6). Right: closed form (PDB 1EX7). Top: standard sketch. Bottom: van-der-Waals spheres. Drawn with Molscript [33].

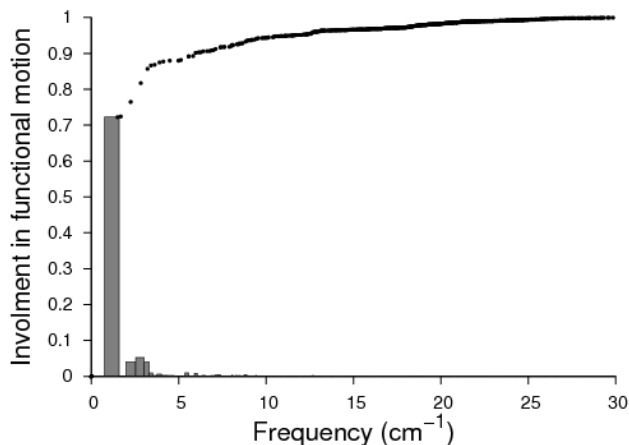


Figure 8: Accuracy of the description of the conformational change of *Saccharomyces cerevisiae* guanylate kinase with low-frequency modes, as obtained using an elastic network model (PDB 1EX6, $R_c = 10$ Å). Boxes: involvement coefficients. Black disks: cumulative sum. The force constant of the springs was chosen so as to have a lowest-frequency of 1.5 cm^{-1} .

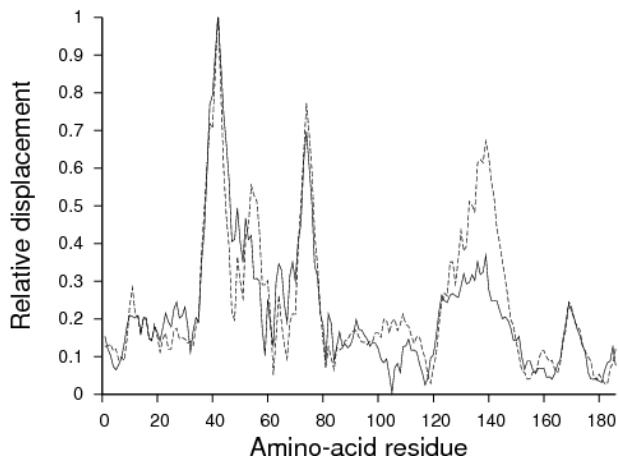


Figure 9: Comparison of the conformational change of *Saccharomyces cerevisiae* guanylate kinase (plain line) with its lowest-frequency mode (dotted line), as obtained using an elastic network model (PDB 1EX6, $R_c = 10$ Å). Both sets of C_α displacements are normalized with respect to the maximum value.

D. Robust modes

However, to turn such a qualitative description into a possibly useful prediction, a way to identify *a priori* the modes the most involved in the functional motion is required. To do so, low-resolution experimental data can prove enough like, for instance, those obtained by cryo-electromicroscopy [40–42]. A more general possibility is to build upon the robustness of these modes, namely, to look for modes that are little sensitive to the protein model used [39]. For instance, instead of setting springs



Figure 10: Conformational change of *Thermus thermophilus* citrate synthase. Top: open form (PDB 1IOM). Bottom: closed form (PDB 1IXE). Drawn with Molscript [33].

between pairs of C_α atoms less than R_c Ångströms away from each other, as above, the springs can be established so that each C_α atom is linked to $\approx n_c$ of its closest neighbors [39]. Then, overlaps between both sets of modes can be obtained (Eq. 4) and when a mode can be described accurately with a small number of modes (Eq. 5) of the other set it is considered to be a robust one. In the case of the open form of guanylate kinase, with $R_c = 10$ Å and $n_c = 10$, the first four modes calculated with $R_c = 10$ Å can be described with less than three modes calculated with $n_c = 10$, while all others need more than eight. Note that the four robust modes thus identified are enough for describing 81% of the closure motion of guanylate kinase (mode two does not contribute at all; see Fig. 8).

The case of guanylate kinase may look too simple, since the functional motion can be correctly guessed just by looking at the structures (see Fig. 7). Interestingly, results obtained with this model system seem to have a general character [39]. For instance, in the case of citrate synthase, it is possible to guess where the active site is and, as a consequence, where the closure motion should occur. However, the structure is more complex (Fig. 10) and it is hardly feasible to decide where are the limits of each structural domain. Nevertheless, results obtained through a normal mode analysis of a C_α -ENM of dimeric citrate synthase are almost as impressive as those obtained for guanylate kinase. Noteworthy, with

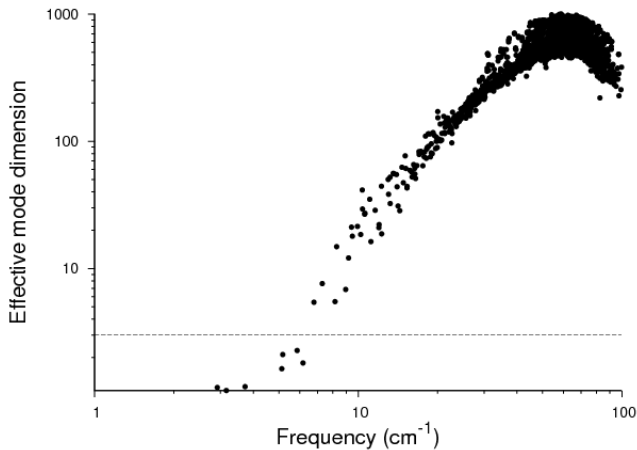


Figure 11: Effective dimension of each eigenvector of dimeric citrate synthase, as obtained with a C_α -ENM (PDB 1IOM; $R_c = 10$). Here, the effective dimension of a mode corresponds to the number of eigenvectors involved in its description, when the later are obtained with $n_c = 10$. The force constant of the springs was chosen so as to have a lowest-frequency of 2.9 cm^{-1} , with $R_c = 10$. The dotted line indicates an effective dimension of three.

$R_c = 10 \text{ \AA}$, $I_2 = 0.29$ and $I_3 = 0.48$, which means that 77% of the conformational change of citrate synthase can be described with these two modes. On the other hand, with $n_c = 10$, $I_2 = 0.27$ and $I_3 = 0.48$. As expected, modes two and three are among the most robust ones. However, in the case of dimeric citrate synthase, there are more than two robust modes. Actually, the first seven modes obtained with $R_c = 10$ can be described accurately with less than three modes obtained with $n_c = 10$ (Fig. 11).

Note that, when compared with modes obtained with $n_c = 10$, high-frequency modes obtained with $R_c = 10$ can certainly not be considered as being robust (their effective dimension is 200 or more; Fig. 11). This is because, as a consequence of the cutoff criterion, such modes correspond to motions of residues belonging to parts of the structure where density (in a coarse-grained sense) is the highest. This is not the case with $n_c = 10$. As a matter of fact, the later kind of ENM was designed so as to show that low-frequency modes do not result from density patterns inside a structure but from mass distribution in space, that is, from the overall shape of the structure [39].

E. Crystallographic B-factors

Having access to an analytical solution of the equations of atomic motion (Eq. 2) allows for the calculation of many quantities [43], like the fluctuations of atomic coordinates around their equilibrium values. For instance,

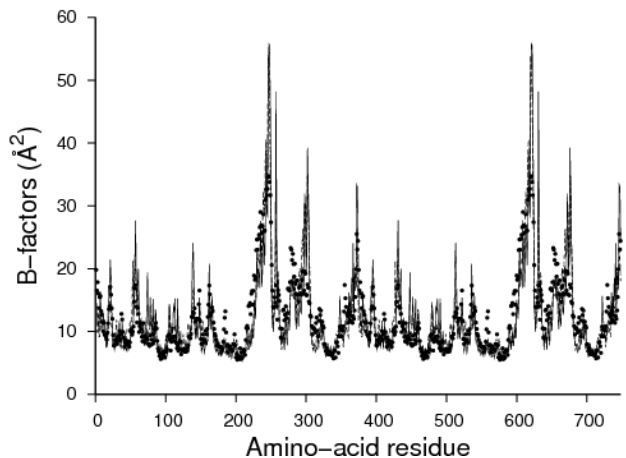


Figure 12: B-factors of dimeric citrate synthase. Filled circles: experimental values (PDB 1IOM). Plain and dotted lines, respectively: values calculated either with a standard ENM ($R_c = 10$) or with $n_c = 10$. Calculated values are shifted and scaled, so that minimum and average values are the same as experimental ones. A justification for such a treatment is that experimental B-factors include various physical effects, other than thermal intra-protein fluctuations.

in the case of the x coordinate of atom i :

$$\langle \Delta x_i^2 \rangle = k_B T \sum_{k=1}^n \frac{a_{ik}^2}{4\pi^2 m_i \nu_k^2} \quad (7)$$

where T is the temperature, k_B , the Boltzman constant, n , the number of modes taken into account ($n = 3N - 6$, unless specified otherwise) and where $\langle \rangle$ denotes a time average. Note that the six rigid-body modes (translation and rotation ones), as a consequence of their null frequencies, are usually excluded from (7).

Interestingly, crystallographic B-factors are expected to derive from the fluctuations of atomic positions within the crystal cell, namely:

$$B_i = \frac{8\pi^2}{3} \langle \Delta x_i^2 + \Delta y_i^2 + \Delta z_i^2 \rangle$$

where B_i is the isotropic B-factor of atom i . Although other factors contribute to the experimental values, such as crystal disorder or phonons, fair correlations have been obtained with values calculated using ENMs [44], especially when effects of neighboring molecules in the crystal are included [45, 46]. Fig. 12 illustrates how accurate B-factors calculated with ENMs can be, even without taking such subtleties into account. Here, the correlation between experimental and calculated values is 0.80, when a cutoff-based ENM is used, and 0.85, when a constant-number-of-neighbors ENM is used. Note that predictions made with both kinds of ENMs are hardly distinguishable. This is a mere consequence of the weight of the low-frequency modes in (7). Indeed, taking into account only the seven robust modes identified previously ($n = 7$) yields a correlation of 0.82, that is, a value as high as when all modes are used ($n = 3N - 6$).

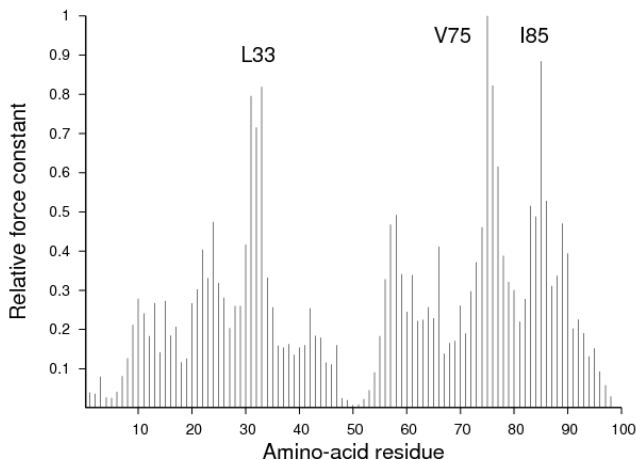


Figure 13: Rigidity of a monomer of the HIV-protease (PDB 1HHP, $R_c = 10$). Effective force constants have been normalized so that the maximum value is one.

F. Flexibility versus rigidity

As briefly discussed in Section III B, while low-frequency modes can provide information on the overall flexibility of a structure, when a cutoff-based C_α -ENM is considered, high-frequency modes pinpoint parts of the structure where amino-acid density is the highest. Though it is tempting to view such parts as being the most rigid ones, the relationship between protein rigidity and density is not expected to be that straightforward. Also, because high-frequency modes are usually localized, several of them need to be considered in order to get a consistent picture of the overall rigidity inside a structure. Unfortunately, selecting the corresponding subset of high-frequency modes in a rigorous way is not that obvious.

Several alternatives have been proposed. For instance, k_i , an effective local force constant associated to atom i , can be defined as follows [47, 48]:

$$k_i = \frac{3k_B T}{\langle (\bar{d}_i - \langle \bar{d}_i \rangle)^2 \rangle}$$

where \bar{d}_i is the average distance of atom i from all other atoms in the structure. Note that it is when this average distance fluctuates little that the force constant (the rigidity) is high. Of course, when the considered protein is a multi-domains one, the average is meaningful only if it is calculated for atoms belonging to the same domain.

Interestingly, this measure involves an ensemble averaging that can be performed using any protein model, *e.g.*, all-atom as well as coarse-grained ones. For instance, a C_α -ENM can be used together with Eq. 2. Fig. 13 shows the result in the case of the HIV protease. Like with the top eigenvector of the adjacency matrix (see Fig. 6), the peptidic stretch nearby G86 is identified as being rigid, but the site now identified as being the most rigid, V75, was not pinpointed by the previous approach.

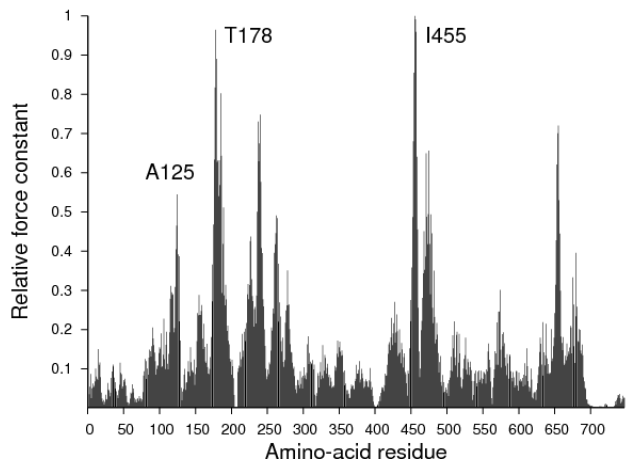


Figure 14: Rigidity of *Dictyostelium discoideum* myosin (PDB 1VOM, $R_c = 10$).

However, V75 is found to be significantly involved in the eigenvector corresponding to the fourth highest eigenvalue of the adjacency matrix. This suggests that when several eigenvectors are taken into account, both methods may provide similar informations about the rigidity of protein structures.

Fig. 14 shows what such an analysis yields in the case of a larger protein, namely, myosin (747 amino-acid residues). Interestingly, T178 and I455, the sites identified as being the most rigid, are both quite close to the enzyme active site, their carbonyl oxygens being 6 and 4Å away, respectively, from phosphate oxygens belonging to the ATP analogue observed in the studied structure (PDB 1VOM).

G. Non-linear network models

Elastic network models have proved useful, in particular because they are very simple. As a consequence, analyses performed with such models can be very quick, allowing for an almost instantaneous check of an hypothesis as well as for large scale studies. However, for many specific applications, ENMs are expected to prove too naive. Therefore, it is of interest to develop more complex models. But, because when complexity increases, the time it takes to perform an analysis usually also does (either for a human being or for a computer), the most useful are expected to be models that are only a bit more complex than ENMs. In practice, since ENMs are, in essence, single-parameter models, increasing their complexity means increasing their number of parameters. So, in order not to increase their complexity too much, a natural choice is to keep the number of parameters as small as possible.

Along this line of thought, in order to recover one of the major property of the potential energy surface of a protein, namely, that it is a multi-minima one, network mod-

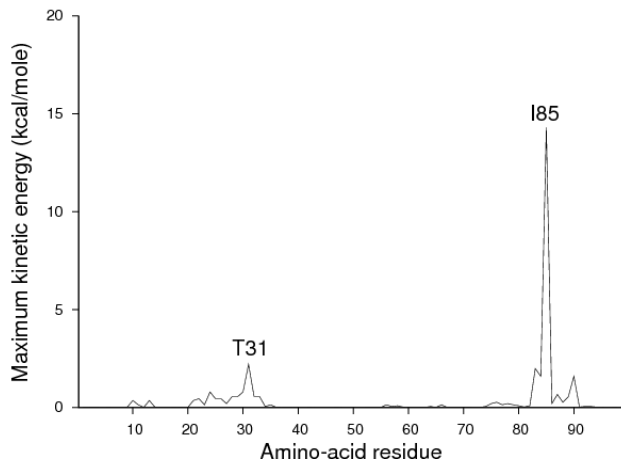


Figure 15: Discrete breather arising from the highest-frequency mode of the HIV-protease (PDB 1HHP, $R_c = 10$). Maximum kinetic energies observed during a 200 ps MD simulation are given, when the highest-frequency mode of the elastic network is excited with 20 kcal/mole.

els with several (usually two) energy minima have been proposed [49, 50]. However, a more basic property of such a surface is that it is highly anharmonic [51, 52]. So, it seems worth starting by adding explicit non-linearity [66] into an elastic network model, *e.g.* [53]:

$$V = \sum_{d_{ij}^0 < R_c} \frac{k_2}{2} (d_{ij} - d_{ij}^0)^2 + \frac{k_4}{4} (d_{ij} - d_{ij}^0)^4 \quad (8)$$

the choice of an additional term with a power of four, instead of three, being mostly for symmetry reasons but also because previous works on one and two-dimensional systems had shown that the dynamical properties of systems with such an energy function can be quite spectacular [54, 55]. Note that when $k_4 = 0$, (8) corresponds to (3), that is, to a standard ENM (up to now, only protein models with $\frac{k_4}{k_2} = 1 \text{ \AA}^2$ have been studied in depth [56]).

One of the dynamical non-linear phenomena that can occur in this context is the birth and the (rather) long-time survival of a discrete breather (DB) [54], that is, a localized mode whose frequency is high enough, so that energy exchange with the rest of the system can prove extremely slow (thousands of periods of the DB). A way to observe such a phenomenon without making any a priori assumption on its nature (localized or not, *etc*) is to perform a molecular dynamics simulation, starting with a high initial temperature and cooling the system through friction on its surface atoms [53]. When a DB sets up, the energy remaining into the system becomes (quite suddenly) localized, the few atoms involved in the DB being the only ones with a significant motion whereas all other ones are almost frozen.

Interestingly, DBs tend to appear in the most rigid parts of a structure [53]. This is due to the fact that most of them are related to one of the high-frequency modes of the elastic network. As a matter of fact, the

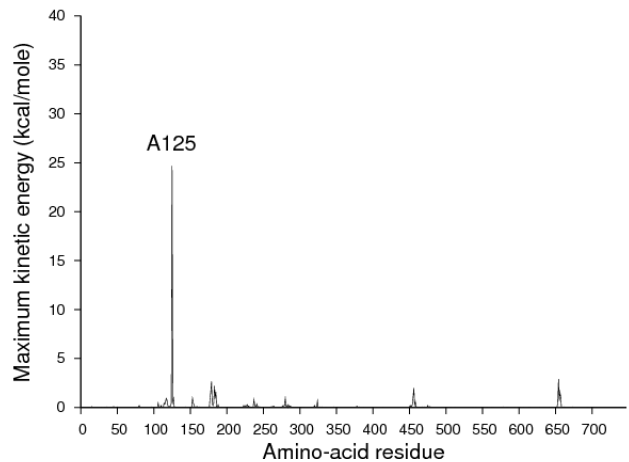


Figure 16: Discrete breather arising from the highest-frequency mode of *Dictyostelium discoideum* myosin (PDB 1VOM, $R_c = 10$). Maximum kinetic energies observed during a 200 ps MD simulation are given, when the highest-frequency mode of the elastic network is excited with 40 kcal/mole.

more energetic a DB is, the higher its frequency [53], the more localized [53, 57] and the more different it is from the high-frequency mode it comes from [57]. As a consequence, a way to obtain DBs is to provide energy to one of the high-frequency modes of the network [58]. Because energetic DBs are highly localized, such a protocol allows to pinpoint a few specific residues (a single one per high-frequency mode [67]).

For instance, in the case of the HIV-protease, exciting the highest-frequency mode highlights residues Ile 85 and Thr 31 (compare Fig. 15 to Figs. 6 and 13) while, in the case of myosin, such an approach highlights residue Ala 125 (see Fig. 16 and compare to Fig. 14). Note that in both cases, more than 50% of the kinetic energy initially given to the highest-frequency mode of the system is observed, during the simulation, on a single residue [68].

IV. CONCLUSION

The study of simple models where a protein is described as a set of Hookean springs linking neighboring amino-acid residues often provides useful informations about its flexibility. Noteworthy, the correlation between calculated residue fluctuations and experimental B-factors can be quite high (Fig. 12). Moreover, in many cases, a few low-frequency modes are found able to provide a fair description of the functional motion of a protein (see Fig. 8 and 9). This is far from being an obvious result since, for instance, the energy function of a set of Hookean springs has a single minimum, while a conformational change is expected to involve (at least) two significantly different minima of the potential energy surface.

Interestingly, modes involved in functional motions

were also found to be robust [39], that is, very little sensitive to changes in the model used to describe the protein. Actually, the robustness of a small subset of the lowest-frequency modes of a protein explains why coarse-grained models can be used on the same footing as highly detailed ones, as far as low-frequency (and large amplitude) motions are concerned. Reciprocally, seeking for robust modes allows to get a small set of coordinates (eigenvectors) able to provide a fair description of the

functional motion a given protein can perform.

More surprisingly, high-frequency modes of cutoff-based elastic networks may also prove useful. Indeed, they pinpoint parts of the structure where the residue density (in a coarse-grained sense) is the highest, and it seems that such parts can be important for the proper folding [32] and/or for the function [35, 48, 53] of many proteins.

-
- [1] Shaw, D. *et al.* Atomic-Level Characterization of the Structural Dynamics of Proteins. *Science* **330**, 341–346 (2010).
- [2] Lindorff-Larsen, K., Piana, S., Dror, R. O. & Shaw, D. E. How fast-folding proteins fold. *Science* **334**, 517–520 (2011).
- [3] Goldstein, H. *Classical Mechanics* (Addison-Wesley, Reading, MA, 1950).
- [4] Wilson, E., Decius, J. & Cross, P. *Molecular Vibrations* (McGraw-Hill, New York, 1955).
- [5] Brooks, B. R. *et al.* CHARMM: A program for macromolecular energy, minimization, and dynamics calculations. *J. Comput. Chem.* **4**, 187–217 (1983).
- [6] Lazaridis, T. & Karplus, M. Effective energy function for proteins in solution. *Proteins* **35**, 133–152 (1999).
- [7] Gerstein, M. & Krebs, W. A database of macromolecular motions. *Nucl. Acid. Res.* **26**, 4280–4290 (1998).
- [8] Brooks, B. R. & Karplus, M. Normal modes for specific motions of macromolecules: application to the hinge-bending mode of lysozyme. *Proc. Natl. Acad. Sci. USA* **82**, 4995–4999 (1985).
- [9] Marques, O. & Sanejouand, Y.-H. Hinge-bending motion in citrate synthase arising from normal mode calculations. *Proteins* **23**, 557–560 (1995).
- [10] Guilbert, C., Perahia, D. & Mouawad, L. A method to explore transition paths in macromolecules. Applications to hemoglobin and phosphoglycerate kinase. *Comp. Phys. Comm.* **91**, 263–273 (1995).
- [11] Thomas, A., Field, M. J., Mouawad, L. & Perahia, D. Analysis of the Low Frequency Normal Modes of the T-state of Aspartate Transcarbamylase. *J. Mol. Biol.* **257**, 1070–1087 (1996).
- [12] Harrison, R. Variational calculation of the normal modes of a large macromolecule: Methods and some initial results. *Biopolymers* **23**, 2943–2949 (1984).
- [13] Mouawad, L. & Perahia, D. DIMB: Diagonalization in a mixed basis. A method to compute low-frequency normal modes for large macromolecules. *Biopolymers* **33**, 569–611 (1993).
- [14] Ghysels, A., Miller, B. T., Pickard, F. C. & Brooks, B. R. Comparing normal modes across different models and scales: Hessian reduction versus coarse-graining. *J. Comp. Chem.* **33**, 2250–2275 (2012).
- [15] Durand, P., Trinquier, G. & Sanejouand, Y. H. A new approach for determining low-frequency normal modes in macromolecules. *Biopolymers* **34**, 759–771 (1994).
- [16] Tama, F., Gadea, F.-X., Marques, O. & Sanejouand, Y.-H. Building-block approach for determining low-frequency normal modes of macromolecules. *Proteins* **41**, 1–7 (2000).
- [17] Gohlke, H. & Thorpe, M. A natural coarse graining for simulating large biomolecular motion. *Biophys. J.* **91**, 2115–2120 (2006).
- [18] Ahmed, A. & Gohlke, H. Multiscale modeling of macromolecular conformational changes combining concepts from rigidity and elastic network theory. *Proteins* **63**, 1038–1051 (2006).
- [19] Elber, R. & Karplus, M. Multiple conformational states of proteins: A molecular dynamics analysis of myoglobin. *Science* **235**, 318–321 (1987).
- [20] Kneller, G. R. & Smith, J. C. Liquid-like side-chain dynamics in myoglobin. *J. Mol. Biol.* **242**, 181–185 (1994).
- [21] Teeter, M., Yamano, A., Stec, B. & Mohanty, U. On the nature of a glassy state of matter in a hydrated protein: relation to protein function. *Proc. Natl. Acad. Sci. USA* **98**, 11242–11247 (2001).
- [22] Ma, J. & Karplus, M. Ligand-induced conformational changes in ras p21: a normal mode and energy minimization analysis. *J. Mol. Biol.* **274**, 114–131 (1997).
- [23] Lamy, A., Souaille, M. & Smith, J. Simulation evidence for experimentally detectable low-temperature vibrational inhomogeneity in a globular protein. *Biopolymers* **39**, 471–478 (1996).
- [24] Batista, P. R. *et al.* Consensus modes, a robust description of protein collective motions from multiple-minima normal mode analysis. Application to the HIV-1 protease. *Phys. Chem. Chem. Phys.* **12**, 2850–2859 (2010).
- [25] Tirion, M. Low-amplitude elastic motions in proteins from a single-parameter atomic analysis. *Phys. Rev. Lett.* **77**, 1905–1908 (1996).
- [26] Bruschiweiler, R. Collective protein dynamics and nuclear spin relaxation. *J. Chem. Phys.* **102**, 3396–3403 (1995).
- [27] Tama, F. & Sanejouand, Y. H. Conformational change of proteins arising from normal mode calculations. *Prot. Engineering* **14**, 1–6 (2001).
- [28] Jacobs, D. J. & Thorpe, M. F. Generic rigidity percolation: the pebble game. *Phys. Rev. Lett.* **75**, 4051–4054 (1995).
- [29] Jacobs, D. J., Rader, A. J., Kuhn, L. A. & Thorpe, M. F. Protein flexibility predictions using graph theory. *Proteins* **44**, 150–165 (2001).
- [30] Haliloglu, T., Bahar, I. & Erman, B. Gaussian dynamics of folded proteins. *Phys. Rev. Letters* **79**, 3090–3093 (1997).
- [31] Kondrashov, D., Cui, Q. & Phillips, G. Optimization and evaluation of a coarse-grained model of protein motion using x-ray crystal data. *Biophys. J.* **91**, 2760–2767 (2006).
- [32] Bahar, I., Atilgan, A. R., Demirel, M. C. & Erman, B. Vibrational dynamics of folded proteins: significance of

- slow and fast motions in relation to function and stability. *Phys. Rev. Lett.* **80**, 2733–2736 (1998).
- [33] Kraulis, P. Molscript: a program to produce both detailed and schematic plots of protein structures. *J. Appl. Cryst.* **24**, 946–950 (1991).
- [34] Hinsen, K. Analysis of domain motions by approximate normal mode calculations. *Proteins* **33**, 417–429 (1998).
- [35] Yang, L. & Bahar, I. Coupling between catalytic site and collective dynamics: a requirement for mechanochemical activity of enzymes. *Structure* **13**, 893–904 (2005).
- [36] Tama, F. & Brooks III, C. The mechanism and pathway of pH induced swelling in cowpea chlorotic mottle virus. *J. Mol. Biol.* **318**, 733–747 (2002).
- [37] Delarue, M. & Sanejouand, Y.-H. Simplified normal modes analysis of conformational transitions in DNA-dependant polymerases: the Elastic Network Model. *J. Mol. Biol.* **320**, 1011–1024 (2002).
- [38] Krebs, W. G. *et al.* Normal mode analysis of macromolecular motions in a database framework: Developing mode concentration as a useful classifying statistic. *Proteins* **48**, 682–695 (2002).
- [39] Nicolay, S. & Sanejouand, Y.-H. Functional Modes of Proteins Are among the Most Robust. *Phys. Rev. Lett.* **96**, 078104 (2006).
- [40] Tama, F., Valle, M., Frank, J. & Brooks III, C. L. Dynamic reorganization of the functionally active ribosome explored by normal mode analysis and cryo-electron microscopy. *Proc. Natl. Acad. Sci. USA* **100**, 9319–9323 (2003).
- [41] Delarue, M. & Dumas, P. On the use of low-frequency normal modes to enforce collective movements in refining macromolecular structural models. *Proc. Natl. Acad. Sci. USA* **101**, 6957–6962 (2004).
- [42] Suhre, K., Navaza, J. & Sanejouand, Y.-H. NORMA: a tool for flexible fitting of high resolution protein structures into low resolution electron microscopy derived density maps. *Act. Cryst. D* **62**, 1098–1100 (2006).
- [43] Bahar, I. & Cui, Q. (eds.). *Normal Mode Analysis: Theory and Applications to Biological and Chemical Systems. C&H/CRC Mathematical & Computational Biology Series, vol. 9* (CRC press, Boca Raton, 2005).
- [44] Bahar, I., Atilgan, A. R. & Erman, B. Direct evaluation of thermal fluctuations in proteins using a single-parameter harmonic potential. *Fold. Des.* **2**, 173–181 (1997).
- [45] Kundu, S., Melton, J., Sorensen, D. & Phillips Jr, G. Dynamics of proteins in crystals: comparison of experiment with simple models. *Biophys. J.* **83**, 723–732 (2002).
- [46] Hinsen, K. Structural flexibility in proteins: Impact of the crystal environment. *Bioinformatics* **24**, 521 (2008).
- [47] Sacquin-Mora, S. & Lavery, R. Investigating the local flexibility of functional residues in hemoproteins. *Biophys. J.* **90**, 2706–2717 (2006).
- [48] Sacquin-Mora, S., Laforet, E. & Lavery, R. Locating the active sites of enzymes using mechanical properties. *Proteins* **67**, 350–359 (2007).
- [49] Maragakis, P. & Karplus, M. Large amplitude conformational change in proteins explored with a plastic network model: adenylate kinase. *J. Mol. Biol.* **352**, 807–822 (2005).
- [50] Chu, J.-W. & Voth, G. A. Coarse-grained free energy functions for studying protein conformational changes: a double-well network model. *Biophys. J.* **93**, 3860–3871 (2007).
- [51] Levy, R., Perahia, D. & Karplus, M. Molecular dynamics of an alpha-helical polypeptide: temperature dependence and deviation from harmonic behavior. *Proc. Natl. Acad. Sci. USA* **79**, 1346–1350 (1982).
- [52] Hayward, S. & Go, N. Collective Variable Description of Native Protein Dynamics. *Annu. Rev. Phys. Chem.* **46**, 223–250 (1995).
- [53] Juanico, B., Sanejouand, Y.-H., Piazza, F. & De Los Rios, P. Discrete breathers in nonlinear network models of proteins. *Phys. Rev. Lett.* **99**, 238104 (2007).
- [54] Flach, S., Kladko, K. & Willis, C. R. Localized excitations in two-dimensional Hamiltonian lattices. *Phys. Rev. E* **50**, 2293–2303 (1994).
- [55] Dauxois, T., Litvak-Hinenzon, A., MacKay, R. & Spanoudaki, A. (eds.). *Energy localisation and transfer in crystals, biomolecules and josephson arrays. Advanced Series in Nonlinear Dynamics, vol.22* (World Scientific, Singapore, 2004).
- [56] Piazza, F. & Sanejouand, Y. H. Breather-mediated energy transfer in proteins. *DCDS-S* **4**, 1247–1266 (2011).
- [57] Piazza, F. & Sanejouand, Y.-H. Discrete breathers in protein structures. *Phys. Biol* **5**, 026001 (2008).
- [58] Piazza, F. & Sanejouand, Y. H. Long-range energy transfer in proteins. *Phys. Biol* **6**, 046014 (2009).
- [59] Li, G. & Cui, Q. A coarse-grained normal mode approach for macromolecules: an efficient implementation and application to Ca(2+)-ATPase. *Biophys. J.* **83**, 2457–2474 (2002).
- [60] Suhre, K. & Sanejouand, Y.-H. Elnémo: a normal mode server for protein movement analysis and the generation of templates for molecular replacement. *Nucl. Ac. Res.* **32**, W610–W614 (2004).
- [61] McCoy, A. J. *et al.* Phaser crystallographic software. *J. Appl. Cryst.* **40**, 658–674 (2007).
- [62] Or on a saddle point.
- [63] This approximation has been implemented in CHARMM under the BNM (Block Normal Modes) acronym [59]. It is used by the Elnémo Web-server [60] as well as by softwares like PHASER [61] and DIAGRTB. The later one is public domain. It can be downloaded at <http://ecole.modelisation.free.fr/modes.html>.
- [64] For its proper folding, in the first place.
- [65] rmsd: root-mean-square deviation.
- [66] Anharmonicity and non-linearity may sound more familiar to, respectively, biophysicists and physicists.
- [67] If the energy provided is high enough.
- [68] The lifetime of these discrete breathers is longer than 200 ps.